Article

ALCAM: A Novel Surface marker on EpCAM[low] Circulating Tumor Cells

Rossana Signorelli [1,2,3]**, Teresa Maidana Giret** [4]**, Oliver Umland** [5]**, Marco Hadisurya**[6]**, Shweta Lavania** [1,2] **, Charles Richard John Lalith**[7]**, Ashley Middleton**[1,2]**, Melinda Minucci Boone**[8]**, Ayse Burcu Ergonul**[8]**, Weiguo Andy Tao**[6]**, Haleh Amirian**[1,2]**, Anton Iliuk**[9]**, Aliya Khan**[10]**, Robert Diaz**[11]**, Daniel Bilbao Cortes**[10,11]**, Monica Garcia-Buitrago**[10,11]**, and Harrys Kishore Charles Jacob** [1,2,10,]***,**

[1] Department of Surgery, University of Miami, Miller School of Medicine, Miami, USA
[2] Sylvester Comprehensive Cancer Center, University of Miami, Miller School of Medicine, Miami, USA
[3] Department of Biology, University of Miami, Miller School of Medicine, Miami, USA
[4] Departments of Radiation Oncology, University of Miami, Miller School of Medicine, Miami, USA
[5] Diabetes Research Institute, University of Miami, Miller School of Medicine, Miami, USA
[6] Department of Biochemistry, Purdue University, West Lafayette, USA
[7] Institute of Engineering in Medicine, University of California San Diego, San Diego, USA
[8] Biospecimen Shared Resource, University of Miami, Miami, USA
[9] Tymora Analytical Operations, Innovations, West Lafayette, USA
[10] Department of Pathology and Laboratory Medicine, University of Miami, Miller School of Medicine, Miami, USA
[11] Sylvester Comprehensive Cancer Center, Cancer Modeling Shared Resource, University of Miami, Miller School of Medicine, Miami, USA

* Correspondence: harryskcjacob@miami.edu; Tel.: +1 786 495 6792

Abstract: Background: Current strategies in circulating tumor cell (CTC) isolation in pancreatic cancer heavily rely on the EpCAM and cytokeratin cell status. EpCAM is generally not considered as a good marker given its transitory change during Epithelial to Mesenchymal Transition (EMT) or reverse EMT. There is a need to identify other surface markers to capture the complete repertoire of PDAC CTCs. The primary objective of the study is to characterize alternate surface biomarkers to EpCAM on CTCs that express low or negligible levels of surface EpCAM in pancreatic cancer patients. **Methods:** Flow cytometry and surface mass spectrometry were used to identify proteins expressed on the surface of PDAC CTCs in culture. CTCs were grown under conditions of attachment and in co-culture with naïve neutrophils. Putative biomarkers were then validated in GEMMs and patient samples. **Results**: Surface proteomic profiling of CTCs identified several novel protein biomarkers. ALCAM was identified as a novel robust marker in GEMM models and in patient samples. Conclusions: We identified several novel surface biomarkers on CTCs expressed under differing conditions of culture. ALCAM was validated and identified as a novel alternate surface marker on EpCAM[low] CTCs.

Keywords: Biomarkers; Pancreatic Cancer; CTC; Surfaceome; Protemics; Flow Cytometry; ALCAM

1. Introduction

Pancreatic cancer has the highest mortality rate among all cancers. For all stages combined, the 5-year survival rate is 11% [1]. Distant organ metastasis is responsible for nearly 90% of cancer associated deaths [2] with the liver and surrounding peritoneum being major sites for metastasis. It has been reported that Circulating Tumor Cells (CTCs), which are disseminated neoplastic cells shed from the primary tumor, have clonal capacity to

reach distant organs and initiate tumor growth [3-5]. Therefore, it is valuable to analyze CTCs to further understand the phenomenon of metastasis. More specifically, in pancreatic ductal adenocarcinoma (PDAC), tumor cells that are shed from the primary site enter the bloodstream, either as singlets or clusters, and promote tumor survival even after surgical resection[4]. CTCs also play an important role in the diagnosis and detection of pancreatic cancer [6-9]; enumeration [10-15] and characterization of CTCs have great potential for clinical prediction, diagnosis, and monitoring in patients with PDAC [16]. CTCs can be conveniently harvested from patients via minimally invasive phlebotomy, however, their rarity among billions of blood cells makes their identification and isolation challenging [7,8]. While recent studies have proposed several advances in instrumentation and strategies to detect CTCs in the blood stream, there has been a heavy dependence on a limited toolbox of markers to characterize these CTCs. The Epithelial Cellular Adhesion Molecule (EpCAM) has been the singular most widely used marker used to separate CTCs; current methods [17-27] employ a positive enrichment strategy to isolate these cells. They are limited to a unique subset of cells in a heterogeneous population of CTCs, either as singlets or as clusters that have high levels of surface EpCAM expression. Methods that do not employ a positive enrichment approach [28-36] and are solely based on physical characteristics of the cells have several issues such as low processing volumes and times in addition to requiring tedious sample fractionation before separation. These different strategies have captured efficiencies ranging anywhere from 11% to 92% [2,8], which still makes it quite a herculean task to capture the complete panorama of CTCs that are released from each cancer type. Currently, the most widely used method for capturing CTCs from PDAC patients has relied heavily on immunocapture techniques that require positively enriching for cells that express cytokeratin and EpCAM and negative for CD45. The lack of appropriate methods to cultivate CTCs *in vitro* poses a major hindering block in characterizing surface or other markers in CTCs.

Therefore, there is an immediate need to identify other surface biomarkers to be used in tandem with EpCAM to capture the complete repertoire of cells in circulation. The present study used flow cytometry and mass spectrometry to identify surface proteins on CTCs that express low or negligible levels of EpCAM. CTCs were cultured under different conditions of attachment and also in co-culture with neutrophils to identify transitory changes on the surface proteome. ALCAM that was identified by both methods was validated in patient samples and shows great promise of being an additional biomarker that can be used for screening CTCs in patients with metastatic pancreatic cancer.

2. Materials and Methods

2.1 Patient Derived Tumor Cell lines

Multiple CTC lines were obtained from Celprogen (Torrance, CA). These cells were labeled with PE conjugated Anti EpCAM. (BioLegend Cat#324206) and analyzed by flow cytometry to determine the level of surface EpCAM. The three selected CTC cell lines (CM61, CF49, and HM59), selected did not have any surface level expression of EpCAM. Cell lines were obtained from the following patients: Caucasian Male aged 61 (CM61), Caucasian Female aged 49 (CF49), and Hispanic Male aged 59 (HM59). CTC cells were isolated from the peripheral blood of PDAC patients with liver metastases (mets). Equal number of cells for each patient were cultured in Medium 106 (Thermo Cat# M106500) with hydrocortisone (1 µg/ml), EGF(10 ng/ml), FGF (10 ng/ml), heparin(10 µg/ml), and 2% FBS and then shifted to a medium with 2% exosome depleted FBS before harvesting for EVs. Cells were cultured under adherent and non-adherent conditions using normal or ultra-low attachment plates respectively to mimic cells in circulation. Cells were also cultured with naïve neutrophils to mimic interactions with blood cells.

2.2 Naïve neutrophil isolation

Naïve neutrophils were isolated from human blood that was collected in EDTA tubes: 50 ml of whole blood was used for each biological replicate. The MACSexpress

whole blood neutrophil isolation kit (Miltenyi Cat#130-104-434) was used to isolate neutrophils. Purity of neutrophils were confirmed by Wright Giemsa staining and flow cytometry. The purity was close to 99% on flow cytometric characterization of CD11b+ cell populations.

2.3. Flow cytometric surface protein characterization

The LEGENDScreen Human PE kit (BioLegend Cat#700007) was used to characterize the cell surface markers expressed on the CTC cell lines. To facilitate the analysis of all three cell lines, CM61 was unlabeled, CF49 was labelled with CellTrace violet (violet, 405nm excitation; filter 450/45), and HM59 with CellTrace far red (red, 638nm excitation, filter 660/20). PE conjugated antibodies (yellow, 561nm excitation, filter 585/42) present in each well assessed the expression values of the cell surface markers. The cells were prepared according to the manufacturer's instructions. The samples were acquired on a Beckman Coulter CytoFlex S equipped with 4 laser lines, 405, 488, 561, and 638nm using a 96-well plate reader. CytExpert 2.3 was used for acquisition of data.

2.4. *Karyotyping*

Conventional methods were followed for identification of G-Banding pattern in the CTCs. The cells were karyotyped at the Cytogenetics and Molecular Diagnostic laboratory and the Pathology Services at the University of Miami, Mailman Center for Child development.

2.5. *Preparation of Surface proteome*

CM61 Cells were cultured either as adherent cultures or on low attachment plates (Corning Cat#CLS3814), following which they were either scraped or pelleted to isolate cells for surface proteome preps. 4x10e7 cells were taken for each prep. CM61 CTC cell line was grown in low attachment plates The cell line was subsequently mixed with naïve neutrophils in a 1:1 ratio in HBSS medium (Thermo Cat#14185052) for 1 hour: the cells were then pelleted and subjected to surface proteome preps. The Pierce Cell Surface Protein Isolation kit (Thermo Cat#89881) was used for all cell proteome labeling and isolation. The media was removed and cells were washed twice with ice cold PBS. Surface proteins were cross linked with Sulpho-NHS-SS-Biotin in ice cold PBS for 30 minutes at 4°C. The reaction was quenched and washed with TBS twice. Cell lysis was done by lysis buffer provided in the kit and cells were sonicated on ice using five one second bursts. Cells were then incubated on ice for 30 minutes and vortexed every 5 minutes for 5 sections. Samples were then centrifuged at 10,000g for 2 minutes at 4°C. The supernatant was incubated with NeutrAvidin agarose slurry and incubated for 60 minutes with end over end mixing using a rotator. The beads were then washed twice after which they were eluted with a buffer containing 8M Urea and 50mM DTT.

2.6. *Preparation of Samples for LC-MS*

The immunoprecipitated samples were processed by Tymora Analytical Operations (West Lafayette, IN). The proteins were incubated at 37°C for 15 min to reduce the Cysteine residues and alkylated by incubation in 100 mM iodoacetamide for 45 min at room temperature and in the dark. The samples were diluted 3-fold with 50 mM triethylammonium bicarbonate and digested with Lys-C (Wako Cat# 121- 05063) at 1:100 (wt/wt) enzyme-to-protein ratio for 3 h at 37°C. The samples were further diluted 3-fold with 50 mM triethylammonium bicarbonate and trypsin was added to a final 1:50 (wt/wt) enzyme-to-protein ratio for overnight digestion at 37°C. After digestion, the samples were acidified with trifluoroacetic acid (TFA) to a pH <3 and desalted using Top-Tip C18 tips (Glygen Cat#NC9980572) according to manufacturer's instructions. A portion of each sample was used to determine peptide concentration using Pierce Quantitative Colorimetric Peptide Assay (Thermo Fisher). The samples were dried completely in a vacuum centrifuge and

stored at -80°C. Based on the concentration, 1.4% of each peptide sample was analyzed by Liquid Chromatography Mass spectrometry (LC-MS).

2.7. *LC-MS/MS Analysis*

Dried peptide and phosphopeptide samples were dissolved in 4.8 µL of 0.25% formic acid with 3% (vol/vol) acetonitrile: 4 µL of each were injected into an EasynLC 1000 (Thermo Fisher Scientific). Peptides were separated on a 45-cm in-house packed column (360 µm OD×75 µm ID) containing C18 resin (2.2 µm, 100 Å; Michrom Bioresources). The mobile phase buffer consisted of 0.1% formic acid in ultrapure water (buffer A) with an eluting buffer of 0.1% formic acid in 80% (vol/vol) acetonitrile (buffer B) run with a linear 60- or 90-min gradient of 6–30% buffer B at flow rate of 250 nL/min. The Easy-nLC 1000 was coupled online with a hybrid high-resolution LTQ-Orbitrap Velos Pro mass spectrometer (Thermo Fisher Scientific). The mass spectrometer was operated in the data-dependent mode, in which a full-scan MS (from m/z 300 to 1,500 with the resolution of 30,000 at m/z 400), followed by MS/MS of the 10 most intense ions [normalized collision energy - 30%; automatic gain control (AGC) - 3E4, maximum injection time - 100 ms; 90 sec exclusion]. To specifically focus on the proteins present only on the surface and to remove all background proteins with cytoplasmic or nuclear localization, the biotin enriched proteome was compared with previously published *in silico* and cell surface protein database [44]. Only bonafide cell surface proteins were considered for further studies.

2.8. *Maxquant Label Free quantitation*

Mass spectrometric raw files were analyzed using the MaxQuant software [45]. Peptides were searched against the human Uniprot FASTA database using the Andromeda search engine [46], integrated into MaxQuant. Oxidation and N-terminal acetylation, P/T/S phosphorylations were set as variable modifications, while carbamidomethyl was fixed. Trypsin was chosen as the digestion enzyme with a maximum of 2 missed cleavages. Identified peptides had an initial precursor mass deviation of up to 6 ppm and a fragment mass deviation of 0.6 Da. The false discovery rate (FDR) for peptides (minimum of 7 amino acids) and proteins was 1%. A reverse sequence database was used in determining the FDR. For label-free protein quantification, only unique peptides were considered. A contaminant database provided by the Andromeda search engine was used. All proteins matching the reverse database or labeled as contaminants were filtered out. Label-free protein quantification (LFQ) values were obtained through MaxQuant quantitative label-free analysis[45].

2.9 *GEMM animal experiments*

The study was conducted with the approval from our Institutional Animal Care and Use Committee (IACUC Protocol number 21-045). Kras[LSL.G12D/+]; p53[R172H/+]; Pdx1Cre[tg/+] (KPC) mice were generated in a mixed background (SvJae/C57Bl6/BalbC). Tumors were allowed to be initiated and develop. Animals were sacrificed at humane endpoint and pancreas and distant organ metastases were collected. Samples were fixed in 10% neutral buffered formalin and processed by conventional methods.

2.10 *CTC and DTC isolation from KPC mice*

Blood and ascitic fluid were collected from at least 10 KPC mice pooled and run separately on Parsortix CTC isolation system (AnglePLC). CTCs were collected after washing and by reverse flush from the cassette. CTC or DTC were then suspended in Matrigel and injected subcutaneously in C57Bl6 mice. Tumors were allowed to develop for a month and, after the animals were euthanized, tumors were collected and processed by conventional methods

2.11. *CTC Immunostaining and enumeration*

Blood samples were processed for enumeration of CTCs as described before [47]. Briefly, an automated round-pore microfilter-based isolation system faCTChecker (Circulogix, Inc, FL), developed specifically to capture CTCs, was used for the isolation of CTCs in this study [48]. A pre- mild formaldehyde-based fixation step was performed before filtration.   After filtration, the cells attached to the filter were washed in 1× PBS (Life Technologies Corp, CA).   Isolated cells were stained using primary mouse anti-human CD45, leucocyte common antigen (Agilent Technologies, catalog no. IR75161-2, clones 2B11 + PD7/26) and rabbit anti-CD166 (1:100, Abcam, catalog no. ab109215, clone EPR2759) antibodies; samples were stained overnight at 4 °C.   After being washed thrice in PBS for 5 minutes each, samples were incubated for 1 hour at room temperature with Alexa Fluor® 680 conjugated goat anti-mouse (1:500, Invitrogen, catalog no. A-21058) and AlexaFluor®594 conjugated goat anti-rabbit (1:500, Invitrogen, catalog no. A-11037) secondary antibodies. Subsequently, cells were incubated for 1 h at room temperature with primary Pan-Keratin (C11) mouse monoclonal antibody Alexa Fluor® 488 conjugate (1:150, Cell Signaling Technology, catalog no. 4523) and primary Pan Cytokeratin mouse monoclonal antibody (AE1/AE3) Alexa Fluor 488 conjugate (1:500, eBioscience™, catalog no. 53-9003-82). After another washing step, slides were cover-slipped using ProLong™ Gold Antifade Mountant containing 4',6-diamidino-2-phenylindole (DAPI), (Life Technologies Corporation, catalog no. P36931) for nuclei staining and imaged on the Olympus VS-120 instrument (Olympus) using a 10X objective. CTCs were then identified using our immunocytochemistry (ICC) criteria (round/ovoid size ≥ 6-mm) as Anti-CD166/ALCAM positive/DAPI positive/CD45 negative and Cytokeratin positive/DAPI positive/CD45 negative cells with additional morphology criteria.
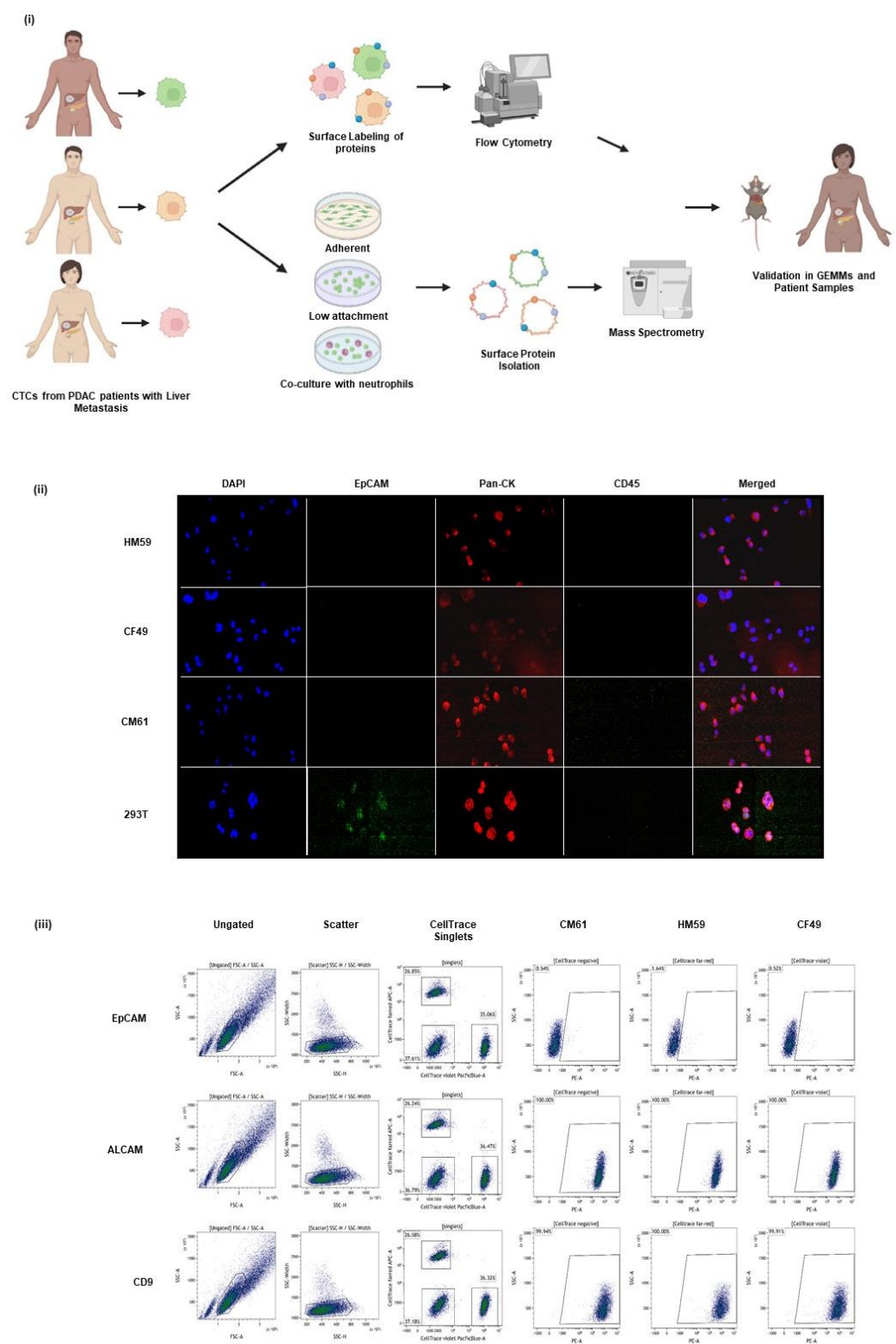
2.12 *Enrichment Analyses*

Reactome [29] and Ingenuity Pathway Analysis [49] were used for enrichment analysis. For Reactome analysis a *pValue* Cutoff of 0.01 or lower was taken to determine statistically significant enrichment of proteins in any pathway being analyzed. GO analysis of identified proteins was done using ShinyGO [50] an FDR cutoff of 0.05 was applied and the top 20 pathways were reported. The pathway analysis was performed in the Ingenuity Pathway Analysis (IPA) for ALCAM. First, the path explorer feature was used to find both direct and indirect paths between the biomarkers and the pathways. Second, the molecule activity predictor (MAP) feature was used to predict the upstream or downstream effects of the upregulated biomarkers.

3. Results

3.1 CTCs express multiple surface proteins that might play a role in pancreatic cancer

Several PDAC CTC cell lines isolated from patients with metastatic cancer were first probed for the expression of surface EpCAM by labeling cells with PE-conjugated anti-EpCAM antibodies. We identified three CTC lines that were negative for EpCAM but were cytokeratin positive. Attentive care was taken to allow for representation across the Hispanic and Caucasian populations: cell lines were taken from a Caucasian female and male patients aged 49 and 61 years respectively as well as from a Hispanic male patient aged 59 years. This assisted with providing an unbiased analysis of surface protein expression across different sample populations. A pipeline of the experimental design of the study is shown in **Figure 1(i)**. These CTC cell lines had a characteristic of differentiating into two subtypes of cells in culture that could not be separated; single cell sorting would eventually give rise to the other cell type. Immunofluorescent labeling of the cells indicated they were CK+/CD45- **[Figure 1(ii)].**

Figure 1. (i) Experimental pipeline indicating CTCs were isolated from peripheral blood of patients. The Cells were either surface labeled to identify proteins by flow cytometry or were cultured under different conditions; as adherent cells or on low attachment plates as single cells or homogenous clusters and as heterogeneous clusters in a co-culture with naïve neutrophils. The surface protein was isolated and subjected to mass spectrometry. (ii) Immunofluorescence labeling of patient isolated CTCs compared with control CTCs stained for DAP1 nuclear stain, EpCAM, Pan-cytokeratin, CD-45 and a merged composite image of all stains combined. (iii) Representative scatter plots for EpCAM, ALCAM and CD9 staining on CTCs that were subjected to flow cytometry. Ungated, scatter, CellTrace plots and individual plots for the CTCs are shown.

These EpCAM negative cells were subjected to further experiments to characterize the surface proteome. A high throughput cytometric screen was done to characterize the surface markers present on all three isolated cell lines. The BioLegend screen contains antibodies against nearly 361 surface proteins alongside respective mouse, rat, or hamster Ig isotype controls. A quick assessment of the cell lines and the repertoire of markers they express *[51]* was analyzed by flow cytometry. For the simultaneous processing of all three cell lines, the individual cell lines were labeled with one of the CellTrace dyes in either the far red, violet spectrum, or left unlabeled. At least 30,000 events were recorded for each marker analyzed in every cell line used in the study. An arbitrary cutoff of being expressed in at least more than 50% in one of the cell lines was followed to identify a candidate list of the top 10 markers expressed across all three cell lines **(Table 1)**. A complete list of all surface markers and their identification percentages across all three CTC lines are analyzed are provided in **Supplementary File S1**. Flow cytometric panels for certain top expressed markers along with their EpCAM status is shown in **Figure 1(iii)**. It is interesting to note that less than 10% of the cells were EpCAM positive and that sorting EpCAM negative cell lines eventually gave rise to a minor EpCAM positive population; this could possibly be associated with the dual cell type populations in the cell lines. We therefore characterized the cell line as EpCAM^{low} even though more than 90% of the cells were EpCAM negative. Therefore, it would be a good starting point to analyze the surface profile of such cells to identify other markers that are expressed at higher levels and can be used in screening cells.

Table 1. Top 10 surface markers expressed on all CTC lines with more than 30% of one of the cell lines expressing the marker. The percentage positive fractions of each CTC line is indicated.

	Protein Marker	Gene Name	Description	CM61 (%+ve)	CF49 (%+ve)	HM59 (%+ve)
1	CD85H	LILRA2	Leukocyte Immunoglobulin-Like Receptor Subfamily A member 2	99.93	100	100
2	CD166	ALCAM	Activated Leukocyte Cell Adhesion Molecule	99.83	99.95	99.98
3	MICA/MICB	MICA/MICB	MHC Class I polypeptide-related sequence A/B	99.90	99.93	99.86
4	CD9	CD9	CD9 antigen	99.73	99.79	99.93
5	EPHA2	EPHA2	Ephrin Type A receptor 2	97.63	99.19	99.16
6	CD252	TNFSF4	Tumor Necrosis Factor Ligand Superfamily member 4	93.08	95.88	97.67
7	CD129	IL9R	Interleukin-9 Receptor	90.50	94.89	93.97
8	CD73	NT5E	5' Nucleotidase	83.43	90.05	90.40
9	CD263	TNFRSF10C	Tumor Necrosis factor receptor superfamily member 10C	67.75	78.85	83.37
10	CD215	IL15RA	Interleukin 15 receptor subunit alpha	60.04	57.96	72.92

IPA analysis of identified surface markers confirmed that these proteins were all plasma membrane associated proteins. Most of the proteins are transmembrane receptors.

Among the other identified types were NT5E, a phosphatase, EPHA2, a kinase, LAMP2, a GPCR, and TNFSF4, an enzyme. A detailed IPA (Qiagen) analysis is shown in **Supplementary File S2**. It is interesting to note that most of the proteins enriched in this analysis are involved in activation of mononuclear leukocytes, blood cells, lymphocytes, or have roles to play in adhesion of/to immune cells and other cell types. These CTC lines show characteristics of leukocyte-like cells, which is consistent with earlier literature of CTCs displaying a hybrid dual positive phenotype [52]. Enrichment of proteins in canonical pathways mediate cross talk between dendritic cells, natural killer cells, and the activation of the JAK1, JAK3, STAT3, and TH2 pathways. A detailed list of enriched canonical pathways is shown in **Supplementary File S2**.

A literature review was also done to assess the role of the identified proteins in pancreatic cancer specifically. In pancreatic cancer, several of the identified proteins have a major role to play in the progression, immune evasion, and resistance to therapy. CD166/ALCAM is a cell adhesion molecule that mediates both heterotypic cell-cell contacts and has been previously shown to promote T cell activation and proliferation. ALCAM positive cells have been shown to be highly tumorigenic in comparison to ALCAM negative cells [53]. Overexpression of ALCAM is also an independent prognosis marker for poor survival and early tumor relapse in PDAC [54] with secreted ALCAM being proposed to be a novel diagnostic marker for pancreatic cancer [55]. MICA and MICB are cell surface proteins, however, unlike canonical class I molecules of the major histocompatibility complex, they do not associate with Beta 2 microglobulin. Levels of MICA/B are also elevated in pancreatic cancer [56] and inhibition of MICA/B, mediated by constitutive activation of the AMPK-GATA2 axis, may serve as a therapeutic target of pancreatic cancer immune evasion [57]. CD9 is another integral membrane protein associated with integrins that regulate processes such as platelet activation and aggregation, cell adhesion, and paranodal junction formality; it has also been shown to be involved in regulating tumor metastasis in several cancers. In PDAC, CD9 positive cells have tumor initiating capacity and give rise to tumor heterogeneity [58] with high levels of expression being strongly associated with poor prognosis [59]. EPHA1 is a receptor tyrosine kinase that promiscuously binds to membrane bound ephrin A family ligands leading to contact dependent bidirectional signaling into neighboring cells. In pancreatic cancer, serum and exosomal levels of EPHA1 family member has been identified to be a potential diagnostic marker for PDAC, complementing CA19-9 and CA242 [60,61]. Moreover, 5'-nucleotidase (NT5E or CD73) is an enzyme that hydrolyzes extracellular nucleotides into membrane permeable nucleosides. It is a glycosylphosphatidylinositol (GPI)-anchored protein that attenuates tumor immunity via cooperation with CD39 to generate immunosuppressive adenosine. Therefore, CD73 may function as a promoter of cancer progression and a regulator in immune patterns [62-64].
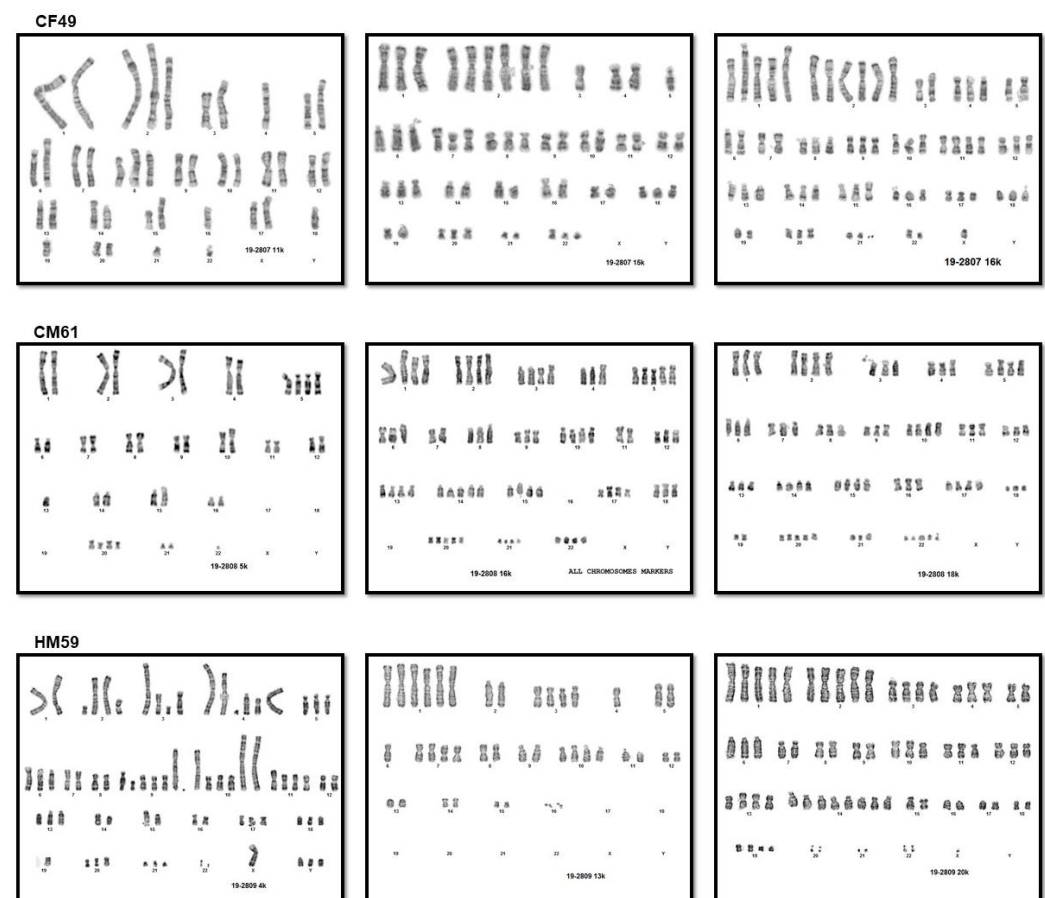
3.2 *Variation in biomarkers on surface could be attributed to the genetic makeup of the CTCs*

In order to analyze whether the changes in expression of the CTCs were due to genetic amplifications or gene rearrangements, a chromosome analysis was performed on 20 G-banded metaphase cells from multiple unstimulated CTC cultures. A G-banding technique was used to analyze all cells. The CF49 cells were analyzed at a banding resolution of 350-400. A total of 20 metaphase cells were analyzed. The majority of the cells showed hypodiploidy. Three cells had a chromosome number in the range of 54-71, a hyperdiploidy to a near-triploidy. All chromosomes were structurally abnormal and the details of the structural changes could not be identified nor described {Cytogenetic result: 37-46[13]/51-76[7]}. HM59 cells were analyzed at a banding resolution of 400-450. A total of 20 metaphase cells were analyzed. The vast majority of the cells in the sample showed hypodiploidy. Three cells had a chromosome number in the range of 69-71, a triploidy or hyper-triploidy. All chromosomes were structurally abnormal and the details of the structural changes could not be identified nor described {Cytogenetic result: 37~44[17]/69~77[3]}. The CM61 cells were analyzed at a banding resolution of 350-400.

There were two cell populations identified in this sample. One population with chromosome numbers in the range of 37-45, showing a so called hypodiploidy in all but one of the cells analyzed. The other population had chromosome numbers in the range of 51-76, resulting in a hyperdiploidy to a near triploidy. All chromosomes were structurally abnormal and details of the structural changes could neither be identified nor described {Cytogenetic result: 37-46[13]/51-76[7]}. Detailed images of the G-banding are shown in **Supplementary Figure S1**. The abnormal chromosomal arrangement in the cells could also be an important factor to consider when analyzing CTCs. In order to prevent biases in contribution of multiple cell types to the proteomics analysis of surface proteins, only the CM61 cell line was taken for all proteomic studies. Differences in expression levels of markers could very well be attributed to gene rearrangements and amplifications.

Supplementary Figure 1. G-Banding karyotyping of CTC cell lines CF49, CM61 and HM59. Metaphase images from at least 5 cells per CTC were taken.

3.3 *CTCs express differing levels of biomarkers on the surface when grown in different culture conditions*

CTCs in circulation are seen either as single cells or clustered with other cell types. Additionally, the LEGENDScreen kit is primarily used to screen cell lines and primary cells (such as PBMCs, bone marrow derived cells, and cells isolated from tissues) for a fixed number of cell surface markers. This kit restricts which markers can be analyzed and therefore limits the potential to identify other surface markers that are more biologically significant. An unbiased mass spectrometric approach was investigated in order to overcome these shortcomings. Since the three cell lines are quite similar in the expression of cell surface markers, the CM61 cell line was used for a detailed characterization of the surface proteome under differing culture conditions. Cells were cultured in low attachment plates as these conditions mimic those seen in in-vivo circulation. Attentive care was taken to avoid breaking up clumps of cells in order to preserve all surface interactions of

the proteins. This was done to mimic homogenous cluster-like conditions in culture. Cells were also cultured in adherent conditions to represent surface markers of cells lines grown on plastic. CTCs are also identified as clusters: to mimic these conditions, a co-culture with naïve neutrophils was also included in the study. For the sake of experimental ease, the CM61 CTC line was grown in low attachment conditions and mixed with equal number of neutrophils. In all cases, the experiment was performed in triplicates in order to show stronger statistically significant data. Surface biotinylation of proteins exposed on the surface was done by labeling cells with EZ-Link Sulfo-NHS-SS-Biotin, which is a thiol-cleavable amine-reactive biotinylation reagent. Cells were subsequently lysed and enriched using NeutrAvidin agarose beads. In order to identify bona fide signal from only the CTCs, and not from the neutrophil contribution, the biotinylated surface proteome of naïve neutrophils was also analyzed. As the individual proteome of each cell type in co-culture was not labeled, attentive care was taken to select only markers that showed changes in expression levels which did not reflect the actual background neutrophil surface markers levels. To achieve this, only a log2FC of more or less than 1.5 fold was considered as actual change attributed to the CTC surface proteome in culture. If a molecule did not satisfy the above mentioned criteria, it was not considered for further analysis. A complete list of molecules identified in all the triplicate mass spectrometric runs is provided in **Supplementary File S3**.

3.3.1 *CTC surface markers differ in cells grown in adherent or low attachment conditions*

A total of 2046 proteins were identified in both conditions with 77 of them being unique to adherent conditions and 52 being unique to low attachment conditions. A log2FC of 1.5 fold was used as an arbitrary cutoff to identify molecules that were expressed either higher or lower in each of the conditions. When comparing the low attachment culture conditions to the adherent culture conditions, we identified 93 proteins that were upregulated in low attachment conditions and 147 proteins that were downregulated in low culture conditions. **Supplementary File S4** provides a list of proteins that were identified in both the adherent and low attachment culture conditions. A Reactome analysis of proteins that were upregulated in the low attachment conditions indicated the neutrophil degranulation, nucleotide savage, and laminin interaction pathways as the top three pathways identified. In addition to this, we also identified proteins that regulate ECM proteoglycans, and RHO GTPase; RAC2; NOTCH pathways. The Reactome analysis was performed with proteins that were downregulated in the low attachment culture condition: the neutrophil degranulation pathway was identified as the most significantly enriched pathway. Additionally, RAB regulation of trafficking, RHOJ and RHO signaling, MET receptor recycling, and Processing of SMDT1 pathway proteins were also identified. A list of all Reactome enriched proteins are provided in **Supplementary File S5**.

3.3.2 *CTC surface markers are differentially regulated on exposure to naïve neutrophils*

CTCs are normally observed as single cells, clusters of cells forming a homogenous population, or heterogeneous clusters with other cells such as neutrophils, platelets, and/or fibroblasts. This cluster association is necessary to evade immune detection and seeding at distant metastatic sites. Earlier studies have looked into transcriptomic changes in CTCs and neutrophils with cell-cell junction and cytokine receptor pairs being identified through transcriptomics [65]. However, not much is known about cell surface receptors on CTCs and how they are modulated when they come in contact with neutrophils. In order to investigate that aspect, CM61, one of the selected CTC cell lines, was cultured in the presence of naïve neutrophils and, subsequently, its surface proteome was examined. Control CTCs were cultured under ultra-low attachment conditions. All experiments were performed to mimic cells in circulation. Furthermore, the surfaceome of naïve neutrophils was taken as a control condition. Only CTCs cultured in low attachment conditions were analyzed for the expression of surface markers.

A total of 2050 proteins were identified in both conditions combined with 80 proteins identified only in neutrophil co-culture and 163 identified only in low attachment conditions. However, upon eliminating proteins that did not show a 1.5 fold difference over expression of the neutrophil surface proteome, only 163 upregulated proteins and 619 downregulated proteins that were in co-culture conditions remained. A Reactome analysis of the upregulated proteins enriched for platelet and neutrophil granulation pathways was performed. Major signaling pathways the proteins enriched for were MAPK oncogenic signaling, MAP2K and MAPK pathways, as well as BRAF and CRAF signaling pathways. Upon CTCs-neutrophils interaction, various pathways were enriched in the downregulated proteins. Some of the top enriched pathways were: the neutrophil degranulation pathway, RHO GTPase pathways, Glucokinase regulation, mitochondrial protein import, VxPx cargo targeting to cilium, protein localization, CDH1 auto-degradation, insulin receptor recycling, and protein folding pathways. A complete list of statistically significant pathways are shown in **Supplementary File S5**.

3.4 *GO analysis indicates a unique repertoire of enrichments in different CTC culture conditions*

GO analysis of proteins in the low attachment CTC culture condition indicated that the upregulated proteins enriched for peptidyl-methionine modifications, negative regulation of cell migration involved in sprouting angiogenesis, positive regulation of TGFβ production, negative regulation of blood vessel endothelial cell proliferation involved in sprouting angiogenesis, and regulation of pattern recognition receptor signaling biological processes to be active. Among the enriched cellular components, the proteins enriched for secretory granule membrane, Ficolin-1 rich granule and its lumen, secretory granules and the tertiary granule membrane. Most proteins were involved in increased aminopeptidase activity, peptidase and endopeptidase activation, IgG binding, SH3 domain binding, and modified amino acid binding.

However, the top biological processes enriched with the downregulated proteins included chylomicron remodeling, hydrogen peroxide metabolic processing, neutrophil activation involved in immune response, protein targeting to mitochondria, and regulation of reactive oxygen species metabolic processing. Cellular enriched components were the chylomicron complex, tertiary, specific, and secretory granule proteins. Very interestingly, the proteins involved with lipase inhibitor activity, Phosphatidylcholine-sterol O-acyltransferase activator activity, cholesterol binding and enzyme regulation were downregulated.

When the same analysis was performed with upregulated proteins in co-culture conditions with naïve neutrophils, the resulting enriched biological processes were proteins involved in NADH regeneration and metabolism, as well as SRP-dependent co-translational proteins targeting the membrane and ER. These proteins belonged to the Ficolin-1 rich granule lumen, cytosolic ribosome, and melanosome cellular components. This could also be indicative of contamination by ribosomal proteins in the immunoprecipitation with beads, which is a very common problem associated with such methods. Proton-transportation of ATP synthase, proton channel activity, and vinculin cadherin and actin filament binding molecular functions were highly enriched. A complete list of statistically significant GO annotations are shown in **Supplementary File S5**.
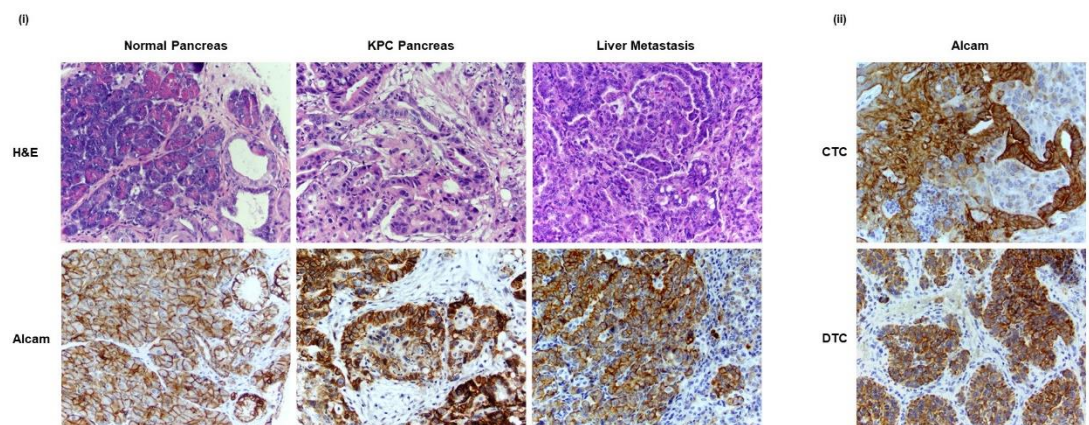
3.5 *CTC marker ALCAM is expressed on CTCs in both GEMM models and in patient samples*

To validate specific markers in animal models, we compared the lists of proteins in both the flow cytometry screen as well as mass spectrometric studies performed on the human CTC lines. We identified Activated Leukocyte Adhesion Molecule (ALCAM) in both these studies. ALCAM is a cell adhesion molecule that is known to mediate both heterotypic cell-cell contacts via interaction with CD6 or by establishing homotypic cell-cell contacts. It is a member of the immunoglobulin receptor subfamily with 5 immunoglobulin-like domains. It has a long extracellular domain (528 Amino acids) with a transmembrane region as well as a short cytoplasmic domain (33 amino acids). There are two known isoforms, "short" and "long", differing in only a stretch of 12 negatively charged

amino acids located in the extracellular domain. The two variants are produced by alternate splicing and are differentially susceptible to cleavage by ADAM metallopeptidase domain 17 or 10 (ADAM17/10) [66,67]. In order to exclude any bias due to cleavage between the long and short isoforms, a specific antibody was used to detect the cytoplasmic domain of ALCAM that is identical between the two isoforms. The marker was expressed on all the three CTC cell lines, and was present in 99% of the cells captured. Additionally, ALCAM was a marker that was overrepresented in CTCs cultured in adherent, low attachment, and co-culture conditions, but minimally expressed on neutrophils, which proves it to be a good marker that could be used in tandem with other CTC markers.

3.5.1 *Alcam is expressed in PDAC GEMM tumors and distant metastatic sites.*

In order to assess, the presence of Alcam in mouse models of cancer, the KPC (Kras[LSL.G12D/+]; p53[R172H/+]; Pdx1Cre[tg/+]) mouse model was utilized as it is an established mouse model of pancreatic cancer. Tissue samples were collected from the primary tumor site and also from distant metastatic site in the spleen, liver, and lungs. In a normal pancreas, Alcam is primarily localized to the cell membrane of the ducts, acini and islet cells. In primary and metastatic PDAC, the localization is shifted to the cytoplasm. The antibody used targeted the cytoplasmic domain of Alcam that recognized both the translated isoforms of Alcam thus providing an unbiased detection of both isoforms **[Figure 2(i)]**. Staining with an antibody that targets the extracellular domain shows similar results (data not shown)

Figure 2. (i) H&E and Alcam staining of pancreas in C57BL6 and KPC GEMM mice with pancreatic cancer. Staining of liver metastasis in KPC GEMM mice (40X magnification). (ii) Alcam staining in Circulating Tumor Cell (CTC) and Dissociated Tumor cells (DTC) that were propagated in subcutaneous models (40X magnification).
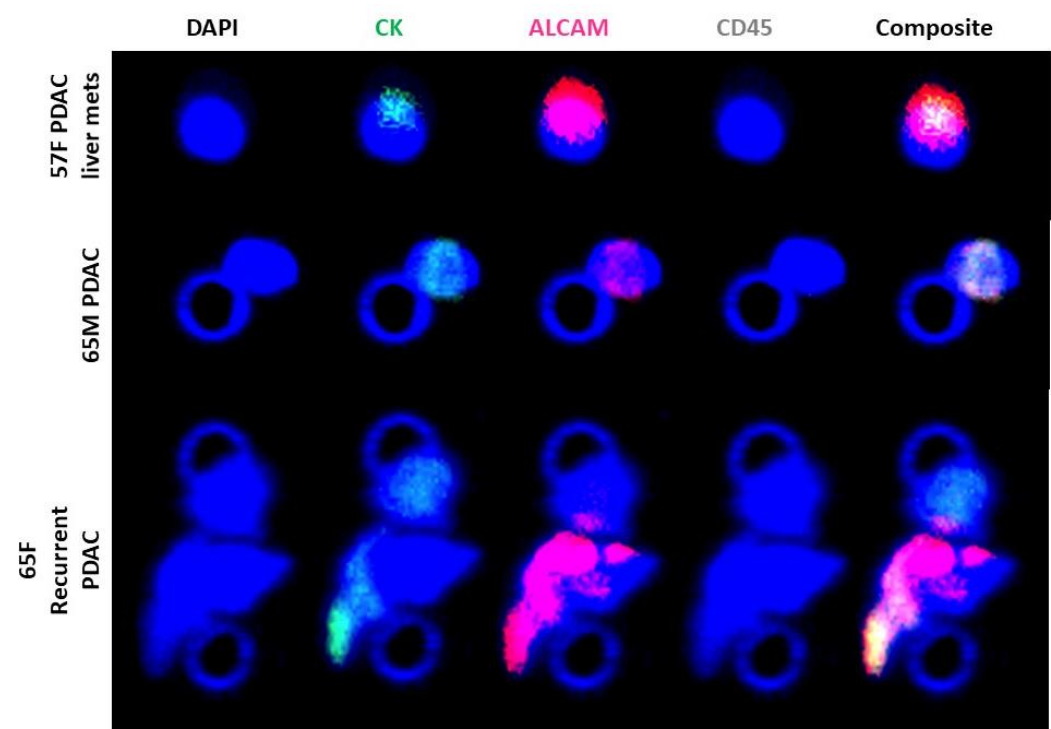
3.5.2 *Alcam is expressed in PDAC GEMM circulating and disseminated tumor cells.*

In order to assess expression of Alcam in the KPC GEMM CTCs, attempts were made to isolate CTCs and Disseminated Tumor cells (DTCs) from blood and ascites respectively. The Parsortix system was used to separate CTCs from the blood. In-cassette staining did not detect any cells and no cells were able to be grown in culture. To circumvent this issue, the isolated CTCs and DTCs were injected subcutaneously in C57Bl6 mice and allowed to form tumors that were then subjected to histochemical analysis for the expression of Alcam **[Figure 2(ii)]**. Interestingly, the CTC and DTC cultures showed membrane and cytoplasmic expression of Alcam; there was very strong staining observed in both the CTC and DTC subcutaneous tumors, which is indicative of Alcam being a very robust marker **[Figure 2(ii)]**.

3.6 *ALCAM is expressed on the surface of CTCs isolated from PDAC patients.*

     To clinically investigate the validity of ALCAM, identified from the screens as a potential marker, samples were collected from peripheral blood of pancreatic cancer patients. Peripheral blood was collected from a 65-year-old male who did not have any chemotherapy and did not have liver mets, a 57-year-old male with PDAC and extensive liver mets, and a 65-year-old female patient with recurrent PDAC. The blood was then parsed through the Parsortix instrument and CTCs were collected. The CTCs were then fixed in formalin and filtered on Circulogix filters and stained for cytokeratin, ALCAM, and CD45 with DAPI as a nuclear stain. We identified a total of 75 single CTCs and 1 cluster from the 57 year old male that were CD45 negative, Cytokeratin positive, and ALCAM positive. On the other hand, in the 65 year old male patient, we identified 31 single CTCs and 2 clusters. In the third patient, with recurrent PDAC, we identified 22 single CTCs and 1 cluster. Representative images of single CTCs and clusters are shown in **Figure 3**. It is important to note that all the CTCs were positive for ALCAM, which is once again indicative of it being a robust marker for detection of PDAC CTC.
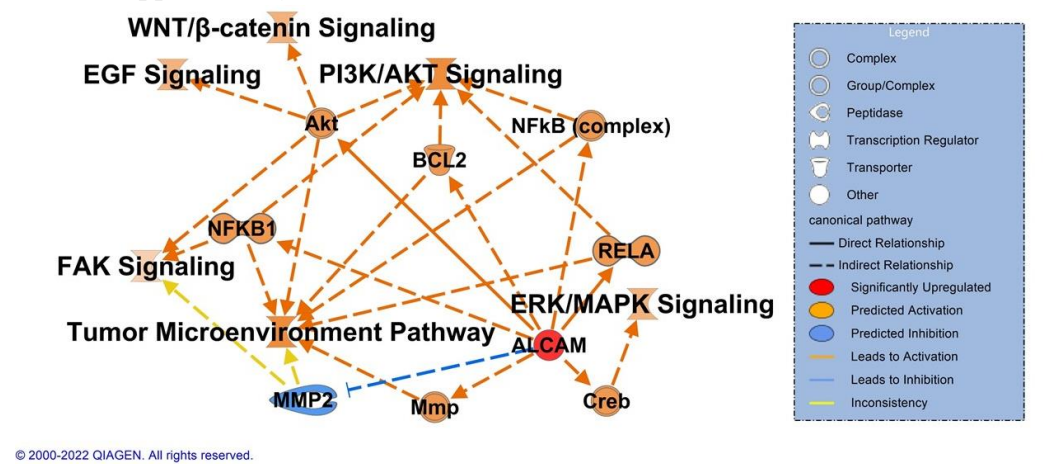

Figure 3. Immunocytochemical staining of CTCs isolated from peripheral blood of patients with pancreatic cancer. CTCs were captured on Circulogix filters and stained for DAPI, Cytokeratin, ALCAM, and CD45 along with a composite image of all stains. Patients are a 57-year-old female with liver mets, second patient is a 65-year-old-male with pancreatic ductal adenocarcinoma and the third patient is a 65-year-old female with a recurrent case of pancreatic ductal adenocarcinoma.

3.7 *ALCAM activates multiple signaling pathways in pancreatic cancer.*

     In order to investigate the role of ALCAM in pancreatic cancer signaling, an IPA Path Designer (Qiagen) analysis was performed. Common pathways that have a role in pancreatic cancer were taken into consideration: the EGF, FAK, WNT/β-catenin, PI3K/AKT, ERK/MAPK, and the tumor microenvironment pathways. Literature review indicates a direct association of ALCAM with increased activity and expression of AKT [68], RELA [69], and CREB [70]. Indirect associations are noted between the NFκB, FAK, PI3K/AKT, WNT-β-catenin, BCL2, and tumor microenvironment pathways. Hypothetical activation of ALCAM results in activation of all the signaling pathways associated with cancer. There is, however, inhibition of MMP2 that could result in activation of FAK signaling pathway or the tumor microenvironment pathway. Nonetheless, this last connec-

tion is inconclusive due to the lack of valid data points to determine its role for the molecule activity prediction algorithm **(Figure 4)**. Enrichment details for pathways are provided in **Supplementary File S6**.

Figure 4. IPA path design with major signaling pathways specific to pancreatic cancer to be upregulated on activation of ALCAM. Solid lines indicate a direct association while dashed lines indicate indirect association with a signaling pathway. Orange denoted activation while blue indicates inhibition and yellow indicates inconsistent relationship or data points to predict the connection between the nodes.

4. Discussion

Pancreatic cancer has defied early detection and can only be detected in advanced stages. It is curable if detected in stage I, provided it is amenable to resection. There is a need for pancreatic cancer CTC specific markers to help increase early detection rates and identify the gamut of cellular subtypes in circulation. In the past, EpCAM and cytokeratin levels have been widely used to identify CTCs. However, EpCAM is generally not a robust marker as there are differing levels of expression based on the EMT status of the cell. Additionally, as shown in this study and others discussed in literature, exposure to neutrophils or other cell types changes the expression of cell surface markers. To identify alternate markers on EpCAM negative or low expressing cells, CTCs were screened for expression of EpCAM; three cell lines were identified in which less than 10% of the cells expressed surface EpCAM. All CTCs analyzed in this study were identified from patients who had metastatic lesions in the liver and were racially diverse, in order to reduce bias on cell surface epitope projection. Additionally, cell lines from both sexes were considered to finally generate a biomarker surface map with minimal bias. To be able to get enough cells for flow cytometry or enough proteins for mass spectrometric analyses, only CTCs that could be cultured and expanded were selected for this study. These CTCs were positive for CA19-9, CEA, Galactosyl transferase II, FAD, Alpa-1-antitrypsin, mucin, CK7, and 3-5% of the cells were also CD133 positive. The flow cytometric screen for surface markers identified a few makers but the original intent of the screen was to quickly characterize the collected blood and cancer cells. It was only through a surface proteomic characterization that we could obtain an unbiased analysis of the CTC cell surface. When CTCs were cultured in adherent and low attachment conditions, most proteins did not change, even though there were differences in some surface proteins. The most drastic difference was observed when a CTC cell line was cultured with naïve neutrophils. An earlier study from our group showed that extracellular vesicles (EVs) secreted from CTCs could induce early granulatory changes in neutrophils [71]. We observed downregulation of nearly 619 proteins: these changes could be initiated due to cell-cell communication between the neutrophils and the CTCs or due to the transfer of EVs from one cell type to another. This is important when it comes to detecting clusters that evade immune detection as it could explain the difference between CTCs associating with other blood cells or even with other

cell types to form clusters. Additionally, these could also be responsible for seeding at distant metastatic sites based on what surface receptors/proteins are present. The circulatory microenvironment with blood cells, immune cells, serum, exosomes from different tissues, growth factors, and other blood constituents complicates the detection of proteins for characterizing patient CTCs. Co-culturing CTCs with other immune or blood cell types could possibly provide additional clues as to what surface proteins would be exposed in heterogeneous clusters. A cytogenetic analysis was also performed to understand the genetic makeup of these cells. There are extensive chromosomal rearrangements and triploidy observed in these culturable CTCs, which is indicative of an increase in marker expression as related to the cellular makeup. Exome sequencing (hybridization based) or solid tumor panel (amplicon based) assays could not provide any suitable results. The generated amplicons did not align well with the target and the majority of the amplicons were on Chromosome 21 (about 95%). No variant or coverage information could be obtained. Therefore, additional experiments need to be done in order to investigate the genetic makeup of these cells.

ALCAM was identified in both screens and it posed as a suitable marker for investigation. However, the role of ALCAM in pancreatic cancer is debated. ALCAM has been detected at the mRNA level in PDAC CTCs in patients after palliative chemotherapy [72]. Nevertheless, we did detect ALCAM in the patient who had recurrent PDAC after their chemotherapeutic regimen. Additionally, there could be differences in the transcription and translation of ALCAM which could explain the behavior as our earlier study only looked at the transcriptional signature and not at the protein level. Moreover, there are two isoforms of the protein that are present: we could overcome the issue by using an antibody that detects the cytoplasmic domain that is identical between the two isoforms. ALCAM has been identified as a good serum *[73]* and prognostic marker *[54]* with ALCAM positive cells being highly tumorigenic and invasive [53,73-77]. Increased expression of ALCAM in PDAC is an independent prognostic marker for poor survival and early tumor relapse [54,78]. Pathway prediction analysis performed prognosticates that ALCAM has a major role to play in activation of all major pancreatic cancer related signaling pathways, making it an important protein to be investigated in CTC panels.

We provide information on novel surface markers on CTCs that express low levels of EpCAM. This would assist in identifying novel classes of CTCs that are negative or express very low levels of EpCAM. In no way, does this study eliminate the need for EpCAM as a marker but rather suggests the use of ALCAM and other surface markers in tandem to better aid in detecting all subtypes of cells in circulation. Further validation of ALCAM is currently being carried out on a larger cohort of patients to ascertain its suitability as a routine CTC marker.

5. Conclusions

We provide, for the first time, a compendium of cell surface markers on PDAC CTCs expressing low or negligible levels of EpCAM, that were cultured in transitory conditions. ALCAM has been identified as a promising PDAC CTC marker that can be used in combination with current epitopes in preclinical and clinical settings.

Supplementary Materials: The following supporting information can be downloaded at: www.mdpi.com/xxx/s1, Supplementary Figure S1: G-Banding karyotyping of CTC cell lines CF49, CM61 and HM59. Metaphase images from at least 5 cells per CTC were taken; Supplementary File S1: LegendScreen result file with percentages of cells expressing nearly 350 surface proteins. The individual cells well labelled with CellTrace dyes to differentiate between the different cell types. title; Supplementary File S2: IPA enrichment analysis of proteins from LegendScreen analysis with common identified receptors and canonical pathways identified among target proteins analyzed; Supplementary File S3: Proteome Discoverer output detailing all identified proteins in surface proteome experiments with cell surface proteins in CM61 cell line cultured under adherent, low attachment, and in culture with neutrophils. Control surface proteins from an empty bead and also neutrophils alone is also provided; Supplementary File S4: Comparative analysis of cell surface proteins in multiple experimental conditions with lists of proteins differentially regulated in unique experi-

mental conditions; Supplementary File S5: Reactome and GO analysis of different proteins identified in every experimental condition with lists of proteins upregulated or downregulated in specific experimental arm; Supplementary File S6: IPA Path design list of molecules and relationships identified in pathways that are modulated by ALCAM.

Author Contributions: "Conceptualization, H.K.C.J; methodology, R.S., T.M.G., O.U., S.L., A.M., M.M.B., B.A.E., W.A.T., A.I., A.K., R.D., D.B.C., H.A., and H.K.C.J; software, M.H., and C.R.J.L.; validation, R.S., T.M.G., O.U., and H.K.C.J; formal analysis, O.U., M.H., C.R.J.L., and H.K.C.J. ; data curation, R.S., T.M.G., S.L., C.R.J.L., M.M.B., A.B.E.,W.A.T., A.I., A.K., and H.K.C.J; writing—original draft preparation, R.S., T.M.G., S.L., M.B-G., and H.K.C.J; pathological examination, M.G-B.; visualization, R.S., T.M.G., O.U., M.B-G., and H.K.C.J; supervision, H.K.C.J; project administration, S.L.; funding acquisition, H.K.C.J.

Institutional Review Board Statement: The study was conducted according to the guidelines of the Declaration of Helsinki and approved by the Institutional Review Board of the Sylvester Comprehensive Cancer Center protocol code 20060858 approved on 6 June 2007.

Informed Consent Statement: Informed consent was obtained from all subjects involved in the study for collection of blood samples for the separation of CTCs. All samples were de-identified at the source.

Data Availability Statement: All mass spectrometry and sequencing raw files along with analyses files have been deposited at BioStudies under the accession number S-BSST861.

Conflicts of Interest: A.I. and W.A.T. are principals at Tymora Analytical. The rest of the authors declare no conflict of interest.

References

1. Menon, R.; Shahin, H. Extracellular vesicles in spontaneous preterm birth. *Am J Reprod Immunol* **2020**, e13353, doi:10.1111/aji.13353.

2. Klein, C.A. Parallel progression of primary tumours and metastases. *Nat Rev Cancer* **2009**, *9*, 302-312, doi:10.1038/nrc2627.

3. Dimitrov-Markov, S.; Perales-Paton, J.; Bockorny, B.; Dopazo, A.; Munoz, M.; Banos, N.; Bonilla, V.; Menendez, C.; Duran, Y.; Huang, L.; et al. Discovery of New Targets to Control Metastasis in Pancreatic Cancer by Single-cell Transcriptomics Analysis of Circulating Tumor Cells. *Mol Cancer Ther* **2020**, *19*, 1751-1760, doi:10.1158/1535-7163.MCT-19-1166.

4. Zhao, X.; Ma, Y.; Dong, X.; Zhang, Z.; Tian, X.; Zhao, X.; Yang, Y. Molecular characterization of circulating tumor cells in pancreatic ductal adenocarcinoma: potential diagnostic and prognostic significance in clinical practice. *Hepatobiliary Surg Nutr* **2021**, *10*, 796-810, doi:10.21037/hbsn-20-383.

5. Arnoletti, J.P.; Reza, J.; Rosales, A.; Monreal, A.; Fanaian, N.; Whisner, S.; Srivastava, M.; Rivera-Otero, J.; Yu, G.; Phanstiel Iv, O.; et al. Pancreatic Ductal Adenocarcinoma (PDAC) circulating tumor cells influence myeloid cell differentiation to support their survival and immunoresistance in portal vein circulation. *PLoS One* **2022**, *17*, e0265725, doi:10.1371/journal.pone.0265725.

6. Moutinho-Ribeiro, P.; Macedo, G.; Melo, S.A. Pancreatic Cancer Diagnosis and Management: Has the Time Come to Prick the Bubble? *Front Endocrinol (Lausanne)* **2018**, *9*, 779, doi:10.3389/fendo.2018.00779.

7. DiPardo, B.J.; Winograd, P.; Court, C.M.; Tomlinson, J.S. Pancreatic cancer circulating tumor cells: applications for personalized oncology. *Expert Rev Mol Diagn* **2018**, *18*, 809-820, doi:10.1080/14737159.2018.1511429.

8. Martini, V.; Timme-Bronsert, S.; Fichtner-Feigl, S.; Hoeppner, J.; Kulemann, B. Circulating Tumor Cells in Pancreatic Cancer: Current Perspectives. *Cancers (Basel)* **2019**, *11*, doi:10.3390/cancers11111659.

9.   Xie, Z.B.; Yao, L.; Jin, C.; Fu, D.L. Circulating tumor cells in pancreatic cancer patients: efficacy in diagnosis and value in prognosis. *Discov Med* **2016**, *22*, 121-128.

10.   van der Toom, E.E.; Groot, V.P.; Glavaris, S.A.; Gemenetzis, G.; Chalfin, H.J.; Wood, L.D.; Wolfgang, C.L.; de la Rosette, J.; de Reijke, T.M.; Pienta, K.J. Analogous detection of circulating tumor cells using the AccuCyte((R)) -CyteFinder((R)) system and ISET system in patients with locally advanced and metastatic prostate cancer. *Prostate* **2018**, *78*, 300-307, doi:10.1002/pros.23474.

11.   Castro-Giner, F.; Scheidmann, M.C.; Aceto, N. Beyond Enumeration: Functional and Computational Analysis of Circulating Tumor Cells to Investigate Cancer Metastasis. *Front Med (Lausanne)* **2018**, *5*, 34, doi:10.3389/fmed.2018.00034.

12.   Paoletti, C.; Miao, J.; Dolce, E.M.; Darga, E.P.; Repollet, M.I.; Doyle, G.V.; Gralow, J.R.; Hortobagyi, G.N.; Smerage, J.B.; Barlow, W.E.; et al. Circulating Tumor Cell Clusters in Patients with Metastatic Breast Cancer: a SWOG S0500 Translational Medicine Study. *Clin Cancer Res* **2019**, *25*, 6089-6097, doi:10.1158/1078-0432.CCR-19-0208.

13.   O'Toole, S.A.; Spillane, C.; Huang, Y.; Fitzgerald, M.C.; Ffrench, B.; Mohamed, B.; Ward, M.; Gallagher, M.; Kelly, T.; O'Brien, C.; et al. Circulating tumour cell enumeration does not correlate with Miller-Payne grade in a cohort of breast cancer patients undergoing neoadjuvant chemotherapy. *Breast Cancer Res Treat* **2020**, *181*, 571-580, doi:10.1007/s10549-020-05658-7.

14.   Ankeny, J.S.; Court, C.M.; Hou, S.; Li, Q.; Song, M.; Wu, D.; Chen, J.F.; Lee, T.; Lin, M.; Sho, S.; et al. Circulating tumour cells as a biomarker for diagnosis and staging in pancreatic cancer. *Br J Cancer* **2016**, *114*, 1367-1375, doi:10.1038/bjc.2016.121.

15.   Yu, J.; Gemenetzis, G.; Kinny-Koster, B.; Habib, J.R.; Groot, V.P.; Teinor, J.; Yin, L.; Pu, N.; Hasanain, A.; van Oosten, F.; et al. Pancreatic circulating tumor cell detection by targeted single-cell next-generation sequencing. *Cancer Lett* **2020**, *493*, 245-253, doi:10.1016/j.canlet.2020.08.043.

16.   Liu, H.; Sun, B.; Wang, S.; Liu, C.; Lu, Y.; Li, D.; Liu, X. Circulating Tumor Cells as a Biomarker in Pancreatic Ductal Adenocarcinoma. *Cell Physiol Biochem* **2017**, *42*, 373-382, doi:10.1159/000477481.

17.   Punnoose, E.A.; Atwal, S.K.; Spoerke, J.M.; Savage, H.; Pandita, A.; Yeh, R.F.; Pirzkall, A.; Fine, B.M.; Amler, L.C.; Chen, D.S.; et al. Molecular biomarker analyses using circulating tumor cells. *PLoS One* **2010**, *5*, e12517, doi:10.1371/journal.pone.0012517.

18.   Miltenyi, S.; Muller, W.; Weichel, W.; Radbruch, A. High gradient magnetic cell separation with MACS. *Cytometry* **1990**, *11*, 231-238, doi:10.1002/cyto.990110203.

19.   Talasaz, A.H.; Powell, A.A.; Huber, D.E.; Berbee, J.G.; Roh, K.H.; Yu, W.; Xiao, W.; Davis, M.M.; Pease, R.F.; Mindrinos, M.N.; et al. Isolating highly enriched populations of circulating epithelial cells and other rare cells from blood using a magnetic sweeper device. *Proc Natl Acad Sci U S A* **2009**, *106*, 3970-3975, doi:10.1073/pnas.0813188106.

20.   Schmidt, T.G.; Skerra, A. The Strep-tag system for one-step purification and high-affinity detection or capturing of proteins. *Nat Protoc* **2007**, *2*, 1528-1535, doi:10.1038/nprot.2007.209.

21.   Xiong, K.; Wei, W.; Jin, Y.; Wang, S.; Zhao, D.; Wang, S.; Gao, X.; Qiao, C.; Yue, H.; Ma, G.; et al. Biomimetic Immuno-Magnetosomes for High-Performance Enrichment of Circulating Tumor Cells. *Adv Mater* **2016**, *28*, 7929-7935, doi:10.1002/adma.201601643.

22.   Sequist, L.V.; Nagrath, S.; Toner, M.; Haber, D.A.; Lynch, T.J. The CTC-chip: an exciting new tool to detect circulating tumor cells in lung cancer patients. *J Thorac Oncol* **2009**, *4*, 281-283, doi:10.1097/JTO.0b013e3181989565.

23.   Stott, S.L.; Hsu, C.H.; Tsukrov, D.I.; Yu, M.; Miyamoto, D.T.; Waltman, B.A.; Rothenberg, S.M.; Shah, A.M.; Smas, M.E.; Korir, G.K.; et al. Isolation of circulating tumor cells using a microvortex-generating herringbone-chip. *Proc Natl Acad Sci U S A* **2010**, *107*, 18392-18397, doi:10.1073/pnas.1012539107.

24.   Adams, A.A.; Okagbare, P.I.; Feng, J.; Hupert, M.L.; Patterson, D.; Gottert, J.; McCarley, R.L.; Nikitopoulos, D.; Murphy, M.C.; Soper, S.A. Highly efficient circulating tumor cell isolation from whole blood and label-free enumeration using polymer-based microfluidics with an integrated conductivity sensor. *J Am Chem Soc* **2008**, *130*, 8633-8641, doi:10.1021/ja8015022.

25.   Jan, Y.J.; Chen, J.F.; Zhu, Y.; Lu, Y.T.; Chen, S.H.; Chung, H.; Smalley, M.; Huang, Y.W.; Dong, J.; Chen, L.C.; et al. NanoVelcro rare-cell assays for detection and characterization of circulating tumor cells. *Adv Drug Deliv Rev* **2018**, *125*, 78-93, doi:10.1016/j.addr.2018.03.006.

26.   Yoon, H.J.; Kim, T.H.; Zhang, Z.; Azizi, E.; Pham, T.M.; Paoletti, C.; Lin, J.; Ramnath, N.; Wicha, M.S.; Hayes, D.F.; et al. Sensitive capture of circulating tumour cells by functionalized graphene oxide nanosheets. *Nat Nanotechnol* **2013**, *8*, 735-741, doi:10.1038/nnano.2013.194.

27.   Yoon, H.J.; Shanker, A.; Wang, Y.; Kozminsky, M.; Jin, Q.; Palanisamy, N.; Burness, M.L.; Azizi, E.; Simeone, D.M.; Wicha, M.S.; et al. Tunable Thermal-Sensitive Polymer-Graphene Oxide Composite for Efficient Capture and Release of Viable Circulating Tumor Cells. *Adv Mater* **2016**, *28*, 4891-4897, doi:10.1002/adma.201600658.

28.   Loeian, M.S.; Mehdi Aghaei, S.; Farhadi, F.; Rai, V.; Yang, H.W.; Johnson, M.D.; Aqil, F.; Mandadi, M.; Rai, S.N.; Panchapakesan, B. Liquid biopsy using the nanotube-CTC-chip: capture of invasive CTCs with high purity using preferential adherence in breast cancer patients. *Lab Chip* **2019**, *19*, 1899-1915, doi:10.1039/c9lc00274j.

29.   Harouaka, R.A.; Zhou, M.D.; Yeh, Y.T.; Khan, W.J.; Das, A.; Liu, X.; Christ, C.C.; Dicker, D.T.; Baney, T.S.; Kaifi, J.T.; et al. Flexible micro spring array device for high-throughput enrichment of viable circulating tumor cells. *Clin Chem* **2014**, *60*, 323-333, doi:10.1373/clinchem.2013.206805.

30.   Farace, F.; Massard, C.; Vimond, N.; Drusch, F.; Jacques, N.; Billiot, F.; Laplanche, A.; Chauchereau, A.; Lacroix, L.; Planchard, D.; et al. A direct comparison of CellSearch and ISET for circulating tumour-cell detection in patients with metastatic carcinomas. *Br J Cancer* **2011**, *105*, 847-853, doi:10.1038/bjc.2011.294.

31.   Zhou, M.D.; Hao, S.; Williams, A.J.; Harouaka, R.A.; Schrand, B.; Rawal, S.; Ao, Z.; Brenneman, R.; Gilboa, E.; Lu, B.; et al. Separable bilayer microfiltration device for viable label-free enrichment of circulating tumour cells. *Sci Rep* **2014**, *4*, 7392, doi:10.1038/srep07392.

32.   Cohen, E.N.; Jayachandran, G.; Hardy, M.R.; Venkata Subramanian, A.M.; Meng, X.; Reuben, J.M. Antigen-agnostic microfluidics-based circulating tumor cell enrichment and downstream molecular characterization. *PLoS One* **2020**, *15*, e0241123, doi:10.1371/journal.pone.0241123.

33.   Hosokawa, M.; Hayata, T.; Fukuda, Y.; Arakaki, A.; Yoshino, T.; Tanaka, T.; Matsunaga, T. Size-selective microcavity array for rapid and efficient detection of circulating tumor cells. *Anal Chem* **2010**, *82*, 6629-6635, doi:10.1021/ac101222x.

34.   Lee, Y.; Guan, G.; Bhagat, A.A. ClearCell(R) FX, a label-free microfluidics technology for enrichment of viable circulating tumor cells. *Cytometry A* **2018**, *93*, 1251-1254, doi:10.1002/cyto.a.23507.

35.   Hyun, K.A.; Kwon, K.; Han, H.; Kim, S.I.; Jung, H.I. Microfluidic flow fractionation device for label-free isolation of circulating tumor cells (CTCs) from breast cancer patients. *Biosens Bioelectron* **2013**, *40*, 206-212, doi:10.1016/j.bios.2012.07.021.

36.   Konigsberg, R.; Obermayr, E.; Bises, G.; Pfeiler, G.; Gneist, M.; Wrba, F.; de Santis, M.; Zeillinger, R.; Hudec, M.; Dittrich, C. Detection of EpCAM positive and negative circulating tumor cells in metastatic breast cancer patients. *Acta Oncol* **2011**, *50*, 700-710, doi:10.3109/0284186X.2010.549151.

37.   Akita, H.; Nagano, H.; Takeda, Y.; Eguchi, H.; Wada, H.; Kobayashi, S.; Marubashi, S.; Tanemura, M.; Takahashi, H.; Ohigashi, H.; et al. Ep-CAM is a significant prognostic factor in pancreatic cancer patients by suppressing cell activity. *Oncogene* **2011**, *30*, 3468-3476, doi:10.1038/onc.2011.59.

38.   Gebauer, F.; Struck, L.; Tachezy, M.; Vashist, Y.; Wicklein, D.; Schumacher, U.; Izbicki, J.R.; Bockhorn, M. Serum EpCAM expression in pancreatic cancer. *Anticancer Res* **2014**, *34*, 4741-4746.

39.   Keller, L.; Werner, S.; Pantel, K. Biology and clinical relevance of EpCAM. *Cell Stress* **2019**, *3*, 165-180, doi:10.15698/cst2019.06.188.

40.   Schnell, U.; Kuipers, J.; Giepmans, B.N. EpCAM proteolysis: new fragments with distinct functions? *Biosci Rep* **2013**, *33*, e00030, doi:10.1042/BSR20120128.

41.   Fong, D.; Moser, P.; Kasal, A.; Seeber, A.; Gastl, G.; Martowicz, A.; Wurm, M.; Mian, C.; Obrist, P.; Mazzoleni, G.; et al. Loss of membranous expression of the intracellular domain of EpCAM is a frequent event and predicts poor survival in patients with pancreatic cancer. *Histopathology* **2014**, *64*, 683-692, doi:10.1111/his.12307.

42.   Schnell, U.; Kuipers, J.; Mueller, J.L.; Veenstra-Algra, A.; Sivagnanam, M.; Giepmans, B.N. Absence of cell-surface EpCAM in congenital tufting enteropathy. *Hum Mol Genet* **2013**, *22*, 2566-2571, doi:10.1093/hmg/ddt105.

43.   Hyun, K.A.; Koo, G.B.; Han, H.; Sohn, J.; Choi, W.; Kim, S.I.; Jung, H.I.; Kim, Y.S. Epithelial-to-mesenchymal transition leads to loss of EpCAM and different physical properties in circulating tumor cells from metastatic breast cancer. *Oncotarget* **2016**, *7*, 24677-24687, doi:10.18632/oncotarget.8250.

44.   Bausch-Fluck, D.; Goldmann, U.; Muller, S.; van Oostrum, M.; Muller, M.; Schubert, O.T.; Wollscheid, B. The in silico human surfaceome. *Proc Natl Acad Sci U S A* **2018**, *115*, E10988-E10997, doi:10.1073/pnas.1808790115.

45.   Cox, J.; Mann, M. MaxQuant enables high peptide identification rates, individualized p.p.b.-range mass accuracies and proteome-wide protein quantification. *Nat Biotechnol* **2008**, *26*, 1367-1372, doi:10.1038/nbt.1511.

46.   Cox, J.; Neuhauser, N.; Michalski, A.; Scheltema, R.A.; Olsen, J.V.; Mann, M. Andromeda: a peptide search engine integrated into the MaxQuant environment. *J Proteome Res* **2011**, *10*, 1794-1805, doi:10.1021/pr101065j.

47.   Lin, H.K.; Zheng, S.; Williams, A.J.; Balic, M.; Groshen, S.; Scher, H.I.; Fleisher, M.; Stadler, W.; Datar, R.H.; Tai, Y.C.; et al. Portable filter-based microdevice for detection and characterization of circulating tumor cells. *Clin Cancer Res* **2010**, *16*, 5011-5018, doi:10.1158/1078-0432.CCR-10-1105.

48.   Williams, A.; Rawal, S.; Ao, Z.; Torres-Munoz, J.; Balic, M.; Zhou, M.D.; Zheng, S.Y.; Tai, Y.C.; Cote, R.J.; Datar, R. Clinical Translation of a Novel Microfilter Technology Capture, Characterization and Culture of Circulating Tumor Cells. *2013 Ieee Point-of-Care Healthcare Technologies (Pht)* **2013**, 220-223.

49.   Kramer, A.; Green, J.; Pollard, J., Jr.; Tugendreich, S. Causal analysis approaches in Ingenuity Pathway Analysis. *Bioinformatics* **2014**, *30*, 523-530, doi:10.1093/bioinformatics/btt703.

50.   Ge, S.X.; Jung, D.; Yao, R. ShinyGO: a graphical gene-set enrichment tool for animals and plants. *Bioinformatics* **2020**, *36*, 2628-2629, doi:10.1093/bioinformatics/btz931.

51.   Bojic, S.; Hallam, D.; Alcada, N.; Ghareeb, A.; Queen, R.; Pervinder, S.; Buck, H.; Amitai Lange, A.; Figueiredo, G.; Rooney, P.; et al. CD200 Expression Marks a Population of Quiescent Limbal Epithelial Stem Cells with Holoclone Forming Ability. *Stem Cells* **2018**, *36*, 1723-1735, doi:10.1002/stem.2903.

52.   Reduzzi, C.; Vismara, M.; Gerratana, L.; Silvestri, M.; De Braud, F.; Raspagliesi, F.; Verzoni, E.; Di Cosimo, S.; Locati, L.D.; Cristofanilli, M.; et al. The curious phenomenon of dual-positive circulating cells: Longtime overlooked tumor cells. *Semin Cancer Biol* **2020**, *60*, 344-350, doi:10.1016/j.semcancer.2019.10.008.

53.   Fujiwara, K.; Ohuchida, K.; Sada, M.; Horioka, K.; Ulrich, C.D., 3rd; Shindo, K.; Ohtsuka, T.; Takahata, S.; Mizumoto, K.; Oda, Y.; et al. CD166/ALCAM expression is characteristic of tumorigenicity and invasive and migratory activities of pancreatic cancer cells. *PLoS One* **2014**, *9*, e107247, doi:10.1371/journal.pone.0107247.

54.   Kahlert, C.; Weber, H.; Mogler, C.; Bergmann, F.; Schirmacher, P.; Kenngott, H.G.; Matterne, U.; Mollberg, N.; Rahbari, N.N.; Hinz, U.; et al. Increased expression of ALCAM/CD166 in pancreatic cancer is an independent prognostic marker for poor survival and early tumour relapse. *Br J Cancer* **2009**, *101*, 457-464, doi:10.1038/sj.bjc.6605136.

55.   Tachezy, M.; Zander, H.; Marx, A.H.; Stahl, P.R.; Gebauer, F.; Izbicki, J.R.; Bockhorn, M. ALCAM (CD166) expression and serum levels in pancreatic cancer. *PLoS One* **2012**, *7*, e39018, doi:10.1371/journal.pone.0039018.

56.   Xu, X.; Rao, G.S.; Groh, V.; Spies, T.; Gattuso, P.; Kaufman, H.L.; Plate, J.; Prinz, R.A. Major histocompatibility complex class I-related chain A/B (MICA/B) expression in tumor tissue and serum of pancreatic cancer: role of uric acid accumulation in gemcitabine-induced MICA/B expression. *BMC Cancer* **2011**, *11*, 194, doi:10.1186/1471-2407-11-194.

57.   Duan, Q.; Li, H.; Gao, C.; Zhao, H.; Wu, S.; Wu, H.; Wang, C.; Shen, Q.; Yin, T. High glucose promotes pancreatic cancer cells to escape from immune surveillance via AMPK-Bmi1-GATA2-MICA/B pathway. *J Exp Clin Cancer Res* **2019**, *38*, 192, doi:10.1186/s13046-019-1209-9.

58. Wang, V.M.; Ferreira, R.M.M.; Almagro, J.; Evan, T.; Legrave, N.; Zaw Thin, M.; Frith, D.; Carvalho, J.; Barry, D.J.; Snijders, A.P.; et al. CD9 identifies pancreatic cancer stem cells and modulates glutamine metabolism to fuel tumour growth. *Nat Cell Biol* **2019**, *21*, 1425-1435, doi:10.1038/s41556-019-0407-1.

59. Lu, W.; Fei, A.; Jiang, Y.; Chen, L.; Wang, Y. Tetraspanin CD9 interacts with alpha-secretase to enhance its oncogenic function in pancreatic cancer. *Am J Transl Res* **2020**, *12*, 5525-5537.

60. Wei, Q.; Zhang, J.; Li, Z.; Wei, L.; Ren, L. Serum Exo-EphA2 as a Potential Diagnostic Biomarker for Pancreatic Cancer. *Pancreas* **2020**, *49*, 1213-1219, doi:10.1097/MPA.0000000000001660.

61. Fan, J.; Wei, Q.; Koay, E.J.; Liu, Y.; Ning, B.; Bernard, P.W.; Zhang, N.; Han, H.; Katz, M.H.; Zhao, Z.; et al. Chemoresistance Transmission via Exosome-Mediated EphA2 Transfer in Pancreatic Cancer. *Theranostics* **2018**, *8*, 5986-5994, doi:10.7150/thno.26650.

62. Chen, Q.; Pu, N.; Yin, H.; Zhang, J.; Zhao, G.; Lou, W.; Wu, W. CD73 acts as a prognostic biomarker and promotes progression and immune escape in pancreatic cancer. *J Cell Mol Med* **2020**, *24*, 8674-8686, doi:10.1111/jcmm.15500.

63. Zhou, L.; Jia, S.; Chen, Y.; Wang, W.; Wu, Z.; Yu, W.; Zhang, M.; Ding, G.; Cao, L. The distinct role of CD73 in the progression of pancreatic cancer. *J Mol Med (Berl)* **2019**, *97*, 803-815, doi:10.1007/s00109-018-01742-0.

64. Nguyen, A.M.; Zhou, J.; Sicairos, B.; Sonney, S.; Du, Y. Upregulation of CD73 Confers Acquired Radioresistance and is Required for Maintaining Irradiation-selected Pancreatic Cancer Cells in a Mesenchymal State. *Mol Cell Proteomics* **2020**, *19*, 375-389, doi:10.1074/mcp.RA119.001779.

65. Szczerba, B.M.; Castro-Giner, F.; Vetter, M.; Krol, I.; Gkountela, S.; Landin, J.; Scheidmann, M.C.; Donato, C.; Scherrer, R.; Singer, J.; et al. Neutrophils escort circulating tumour cells to enable cell cycle progression. *Nature* **2019**, *566*, 553-557, doi:10.1038/s41586-019-0915-y.

66. Iwagishi, R.; Tanaka, R.; Seto, M.; Takagi, T.; Norioka, N.; Ueyama, T.; Kawamura, T.; Takagi, J.; Ogawa, Y.; Shirakabe, K. Negatively charged amino acids in the stalk region of membrane proteins reduce ectodomain shedding. *J Biol Chem* **2020**, *295*, 12343-12352, doi:10.1074/jbc.RA120.013758.

67. Micciche, F.; Da Riva, L.; Fabbi, M.; Pilotti, S.; Mondellini, P.; Ferrini, S.; Canevari, S.; Pierotti, M.A.; Bongarzone, I. Activated leukocyte cell adhesion molecule expression and shedding in thyroid tumors. *PLoS One* **2011**, *6*, e17141, doi:10.1371/journal.pone.0017141.

68. Ma, L.; Wang, J.; Lin, J.; Pan, Q.; Yu, Y.; Sun, F. Cluster of differentiation 166 (CD166) regulated by phosphatidylinositide 3-Kinase (PI3K)/AKT signaling to exert its anti-apoptotic role via yes-associated protein (YAP) in liver cancer. *J Biol Chem* **2014**, *289*, 6921-6933, doi:10.1074/jbc.M113.524819.

69. Wang, J.; Gu, Z.; Ni, P.; Qiao, Y.; Chen, C.; Liu, X.; Lin, J.; Chen, N.; Fan, Q. NF-kappaB P50/P65 hetero-dimer mediates differential regulation of CD166/ALCAM expression via interaction with micoRNA-9 after serum deprivation, providing evidence for a novel negative auto-regulatory loop. *Nucleic Acids Res* **2011**, *39*, 6440-6455, doi:10.1093/nar/gkr302.

70. Bosserhoff, A.K.; Hofmeister, S.; Ruedel, A.; Schubert, T. DCC is expressed in a CD166-positive subpopulation of chondrocytes in human osteoarthritic cartilage and modulates CRE activity. *Int J Clin Exp Pathol* **2014**, *7*, 1947-1956.

71. Charles Jacob, H.K.; Charles Richard, J.L.; Signorelli, R.; Kashuv, T.; Lavania, S.; Vaish, U.; Boopathy, R.; Middleton, A.; Boone, M.M.; Sundaram, R.; et al. Modulation of Early Neutrophil Granulation: The Circulating Tumor Cell-Extravesicular Connection in Pancreatic Ductal Adenocarcinoma. *Cancers (Basel)* **2021**, *13*, doi:10.3390/cancers13112727.

72. Amantini, C.; Morelli, M.B.; Nabissi, M.; Piva, F.; Marinelli, O.; Maggi, F.; Bianchi, F.; Bittoni, A.; Berardi, R.; Giampieri, R.; et al. Expression Profiling of Circulating Tumor Cells in Pancreatic Ductal Adenocarcinoma Patients: Biomarkers Predicting Overall Survival. *Front Oncol* **2019**, *9*, 874, doi:10.3389/fonc.2019.00874.

73. Hong, X.; Michalski, C.W.; Kong, B.; Zhang, W.; Raggi, M.C.; Sauliunaite, D.; De Oliveira, T.; Friess, H.; Kleeff, J. ALCAM is associated with chemoresistance and tumor cell adhesion in pancreatic cancer. *J Surg Oncol* **2010**, *101*, 564-569, doi:10.1002/jso.21538.

74.   Ni, C.; Zhang, Z.; Zhu, X.; Liu, Y.; Qu, D.; Wu, P.; Huang, J.; Xu, A.X. Prognostic value of CD166 expression in cancers of the digestive system: a systematic review and meta-analysis. *PLoS One* **2013**, *8*, e70958, doi:10.1371/journal.pone.0070958.

75.   Tachezy, M.; Zander, H.; Marx, A.H.; Gebauer, F.; Rawnaq, T.; Kaifi, J.T.; Sauter, G.; Izbicki, J.R.; Bockhorn, M. ALCAM (CD166) expression as novel prognostic biomarker for pancreatic neuroendocrine tumor patients. *J Surg Res* **2011**, *170*, 226-232, doi:10.1016/j.jss.2011.06.002.

76.   Jin, U.H.; Karki, K.; Kim, S.B.; Safe, S. Inhibition of pancreatic cancer Panc1 cell migration by omeprazole is dependent on aryl hydrocarbon receptor activation of JNK. *Biochem Biophys Res Commun* **2018**, *501*, 751-757, doi:10.1016/j.bbrc.2018.05.061.

77.   Zhang, W.W.; Zhan, S.H.; Geng, C.X.; Sun, X.; Erkan, M.; Kleeff, J.; Xie, X.J. Activated leukocyte cell adhesion molecule regulates the interaction between pancreatic cancer cells and stellate cells. *Mol Med Rep* **2016**, *14*, 3627-3633, doi:10.3892/mmr.2016.5681.

78.   Yang, Y.; Sanders, A.J.; Ruge, F.; Dong, X.; Cui, Y.; Dou, Q.P.; Jia, S.; Hao, C.; Ji, J.; Jiang, W.G. Activated leukocyte cell adhesion molecule (ALCAM)/CD166 in pancreatic cancer, a pivotal link to clinical outcome and vascular embolism. *Am J Cancer Res* **2021**, *11*, 5917-5932.